Applied Physics B (2024) 130:84
https://doi.org/10.1007/s00340-024-08221-0

Applied Physics B
Lasers and Optics

RESEARCH

Investigation of the few-mode ytterbium-erbium doped fiber amplifier including effects of ion clustering and secondary energy transfer

Foat R. Iakupov[1] · Maksim A. Chernikov[2] · Andrey I. Baranov[2] · Renat I. Shaidullin[3]

Received: 2 December 2023 / Accepted: 12 April 2024 / Published online: 3 May 2024

Abstract
The complete computational model of a low-mode ytterbium-erbium doped fiber amplifier, based on the numerical analysis of rate equations, was developed. In contrast to existing models, we considered the effects of the secondary energy transfer and the upconversion as well as the presence of isolated ytterbium ions and clustered erbium ions in the aggregate. In addition, the presence of several transverse modes and the effect of transverse spatial hole burning were took into account, too. Necessary parameters of the active medium were determined experimentally by measuring the luminescence decay of active ions and the output power and optical spectrum of a fiber amplifier. The proposed model allows one to calculate both the power and spectral characteristics of ytterbium-erbium doped fiber amplifiers, and the nonstationary dynamics of the population inversion and the luminescence of active ions. This can help one to select the required concentrations of active ions, the geometry and the length of active fibers for each specific task.

1 Introduction

Infrared laser radiation is widely applied in various fields nowadays: materials processing technologies, fiber communication systems, scientific applications. In particular, the wavelength range near 1.5 μm is of special interest due to a number of reasons. First, radiation in this range can be considered as "eye-safe". Second, fused silica exhibits minimum optical losses near 1.55 μm, which is very important for fiber optic communication. Third, Er (erbium) ions have a wide luminescence spectrum in this wavelength range.

Amplifiers and laser sources based on active optical fibers doped with Yb (ytterbium) and Er ions (YEDFA) are often used to generate radiation in this wavelength range. The presence of Yb ions suppresses the effect of concentration quenching of Er and makes it possible to increase considerably the concentration of Er ions without reducing the generation efficiency [1, 2]. Moreover, it makes it possible to increase the efficiency of absorption in the wavelength range near 970 nm, which allows the use of the high-power gallium arsenide diode lasers for pumping. Pump radiation is absorbed by Yb ions, and then the excitation energy is transferred through dipole–dipole interaction to unexcited Er ions (further we will call this effect first energy transfer). Er ions, in turn, nonradiatively relax to a metastable energy level. However, Er ions (unlike Yb) have a large number of energy levels. This leads to the manifestation of the following processes: the energy transfer from an excited Er ion to another excited Er ion (upconversion) [3–5]; the energy transfer from excited Yb ions to excited Er ions (secondary energy-transfer) [6]; the absorption of pump or generated photons by excited Er ions (excited state absorption) [7]. These effects result in the transition of excited Er ions to higher energy levels, what leads to additional losses in terms of signal amplification and generation efficiency.

There are a number of papers that present YEDFA models, for example [8], based on the solution of the rate equations—the evolution of radiation intensity and the energy levels population of Yb and Er ions. In [9] particle swarm optimization method combined with rate equations was used to recover the spectroscopic parameters and the optimum design of YEDFA's. The model included the first and secondary energy transfer between Yb^{3+} and Er^{3+} ions, the

✉ Foat R. Iakupov
iakupov.fr@phystech.edu

[1] Moscow Institute of Physics and Technology (National Research University), Dolgoprudnyy, Russia

[2] NTO "IRE-Polus", Fryazino, Russia

[3] Fryazino Branch of the Kotelnikov Institute of Radioengineering and Electronics RAS, Fryazino, Russia

amplified spontaneous emission and the upconversion and cross relaxation mechanisms among the Er^{3+} ions. The proposed algorithm has been employed to optimize the amplifier performance evaluating the fiber length, input pump and signal power in order to maximize the power conversion efficiency. In [10] the influence of thermal effects on YEDFA performance was investigated using multiphysics model based on combined nonlinear rate equations and heat conduction equation.

However, several significant effects are not taken into account. For example, when a certain concentration level of Yb ions is achieved, some of them become isolated and weakly interact with Er ions [6, 11]. The absorption of pump radiation by such ions does not provide the excitation transfer to Er ions, resulting in the reduction of the generation efficiency. The authors of the paper [6] by measuring the luminescence decay of the Yb and Er ions estimated that the portion of isolated Yb ions was about 15% for concentrations of Yb and Er ions 24×10^{25} m3 and 2×10^{25} m^3, respectively.

Another significant problem is the clustering of Er ions, i.e. the formation of groups of Er ions actively interacting with each other [2, 4]. In such clusters, the upconversion rate is much higher, which further reduces the generation efficiency. In the paper [4], the degree of clustering was measured in aluminosilicate fibers doped with Er ions, by means of the analysis of the amplifier transmission saturation effect. It ranged from 0.4 to 12% depending on the concentration of Er ions. In phosphosilicate fibers this effect is actually stronger: the degree of clustering can vary from 8 to 20% depending on the concentrations of Er and Yb ions [2]. Despite the problem of clustered Er ions is described in the literature, it was not included in a model of the Yb/Er-doped medium so far.

Most of the presented YEDFA models consider only the single-mode operation of the amplifier. However, in a number of cases it is necessary to apply a few-mode (in our work it was assumed that term "few-mode" denote 2–10 transverse LP modes) or even multimode amplifier, using fibers with a larger core diameter, since much higher power can propagate in such fibers without reaching the threshold of various nonlinear effects. Also, in fiber-optic communications the use of the mode division multiplexing (MDM) can significantly increase the data transmission rate [12], because in such case each transverse mode can represent a separate channel. Although there are some papers [10] where multimode propagation was considered, too.

In this paper, we propose the most complete and universal model of the operation of a few-mode YEDFA, which includes clustered Er ions and isolated Yb ions. A number of experiments were also carried out, allowing us to determine the key parameters of the active medium: the coefficients of the first energy transfer C_{ET}, the secondary energy-transfer C_{SET} and the upconversion C_{UC}, as well as the degree of clustering of Er ions and the fraction of isolated Yb ions.

2 Theoretical analysis

2.1 Energy levels of Yb and Er ions

The model of the Yb/Er active medium includes the energy levels $^2F_{7/2}$ and $^2F_{5/2}$ of Yb ions and $^4I_{15/2}$, $^4I_{13/2}$, $^4I_{11/2}$ of Er ions (see Fig. 1), which are numbered from 0 to 4, respectively. Absorption and emission of photons by Yb ions (transitions between ground $^2F_{7/2}$ and metastable $^2F_{5/2}$ levels) are described by the corresponding absorption σ_{01} and emission σ_{10} cross sections. Absorption and emission of photons by Er ions (transitions between $^4I_{15/2}$ and metastable $^4I_{13/2}$ levels) are described by the corresponding absorption σ_{23} and emission σ_{32} cross sections. The transition probabilities A_{ij} describe the spontaneous transitions of active ions from ith to jth energy level. N_i is a total concentration of active ions on ith level.

The first energy transfer from Yb ions to unexcited Er ions is characterized by the coefficient C_{ET}. In addition, a reverse energy transfer from Er ions to Yb ions is also possible. It is assumed [6], that the reverse transfer coefficient is equal to the direct C_{ET} coefficient with high accuracy. We should also take into account the processes of upconversion (described by C_{UC} coefficient) and the secondary energy-transfer (described by C_{SET} coefficient). It is indicated in the literature, that ESA (absorption of laser radiation by excited Er ions) mainly occurs in the case the pump wavelengths are near 980 nm or the generated wavelength exceeds 1590 nm [7]. Since these conditions were not met in the investigated amplifier, ESA effect is not taken into account in our work.

Alike the paper [6], the model includes isolated Yb ions that don't interact with Er ions. Therefore, its effective lifetime in the excited state is much longer. In addition, the clustering of Er ions is also taken into account. It was assumed, that all clusters consist of two ions. This is valid in the case the concentration of Er ions is below 10^{26} m^{-3} [2], whereas the investigated fiber had Er concentration of $\sim1.3\times10^{25}$ m^{-3}. Er clusters are considered as a single item for which only two states are possible: (1) both ions are at $^4I_{15/2}$ energy level; (2) one ion is at $^4I_{15/2}$ energy level and the other one is at $^4I_{13/2}$ energy level. If both Er ions are at $^4I_{13/2}$ energy level, the upconversion process occurs almost instantaneously, meaning that one of the ions transits to $^4I_{15/2}$ level.

So that, the following types of ions are included in the model:

- Isolated Yb ions (concentration $\overline{N}_{Yb}(r)$), not interacting with Er ions;

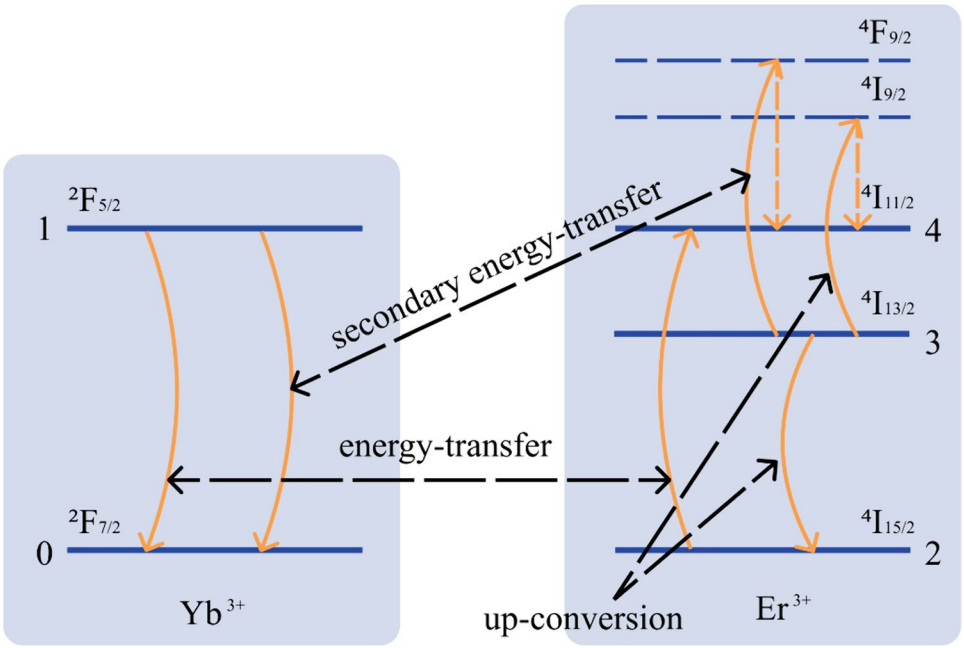

Fig. 1 Energy levels of Yb and Er ions and excitation mechanisms of Er ions. $^4F_{9/2}$ and $^4I_{9/2}$ levels of Er ions are shown, but have not been taken into account in the model

- Non-isolated Yb ions (concentration $\overline{N}_{Yb}(r)$), interacting with non-clustered Er ions (concentration $\hat{N}_{Er}(r)$);
- Non-isolated Yb ions (concentration $\check{N}_{Yb}(r)$), interacting with clustered Er ions (concentration $\check{N}_{Er}(r)$).

The clustering degree can be introduced as:

$$k_{Cl} = \check{N}_{Er}/\hat{N}_{Er} + \check{N}_{Er} \approx \check{N}_{Yb}/\hat{N}_{Yb} + \check{N}_{Yb}. \quad (1)$$

Here, it is assumed that each Er ion interacts approximately with the same number of Yb ions, because they have identical doping profile and constant concentration ratio throughout the volume of active core. So, the share of clustered Er ions is the same as the share of non-isolated Yb ions interacting with it.

2.2 Electromagnetic analysis

The model assumes that the optical pump, which is introduced through the fiber cladding from semiconductor laser diodes, propagates in the form of a large number of transverse modes, so it almost uniformly fills the waveguide. So, the mode distribution function of the pump radiation is $f_{pump}(r) = 1/(\pi(r_{clad})^2)$ in the silica cladding of the active step-index fiber (r_{clad} is the cladding radius), and it is equal to zero outside. For the amplified spontaneous emission (ASE) of Yb ions, that propagates in the active fiber core, the mode distribution function is $f_{aseYb}(r) = 1/(\pi(r_{core})^2)$, where r_{core} is the radius of the optical fiber core. We can use this simplification, since for radiation at wavelengths near 1 μm the investigated fiber can be considered as multimode (more details are given in Sect. 3). In this case, the normalization condition is satisfied for pump and ASE of Yb ions radiation:

$$\int_0^{+\infty} f_{pump/aseYb}(r) \times 2\pi r dr = 1. \quad (2)$$

Then the relationship between optical intensity I and power P has the following form: $I(r, z, \lambda) = f_{pump/aseYb}(r) \times P(z, \lambda)$, where $f_{pump/aseYb}$ is the radial distribution of intensity. The power of spontaneously emitted by Yb ions photons per unit length (for multimode case), which start to propagate along the fiber in forward or backward direction, has the following form [13]:

$$\frac{\partial P_{seYb}^{f/b}}{\partial z} = 4\pi hc^2 \sigma_{10} \frac{\delta\lambda}{\lambda^5} ndn \int_0^{r_{Core}} N_1(r) \times 2\pi r dr. \quad (3)$$

Here n—refractive index of fused silica, dn—refractive index difference between the core and the cladding of the fiber.

For the description of the propagation of signal radiation and amplified spontaneous emission of Er ions it is necessary to consider separately the evolution of each transverse LP mode of the fiber. The number of supported modes in the fiber under study is 6, as was calculated basing on well known solution of eigenvalue equation [14] for an optical fiber with a step refractive index profile. Therefore, the signal emission at a given wavelength λ is described by the array of intensities $\boldsymbol{I}(r,z,\lambda) = \{\ldots, I_m(r, z, \lambda), \ldots\}$ and powers $\boldsymbol{P}(z,\lambda) = \{\ldots, P_m(z,\lambda), \ldots\}$. Here m is the serial number of the mode in the range from 1 to M,

where M is the number of transverse LP modes supported by the fiber. The elementwise ratio between $\boldsymbol{P}$ and $\boldsymbol{I}$ is defined by the array $\boldsymbol{f}_{Er}(r, \lambda) = \{\ldots, f^{Er}{}_m(r, \lambda), \ldots\}$, which elements determine the radial distribution of each transverse mode. This approach allows us to take into account the effect of transverse spatial hole burning in the model.

The power per unit length of photons, spontaneously emitted by Er ions, which start to propagate along the fiber in forward or backward direction, has the following form [13]:

$$\frac{\partial \boldsymbol{P}^{\mathrm{f/b}}_{\mathrm{seEr}}}{\partial z} = \boldsymbol{K} \times hc^2 \sigma_{32} \frac{\delta\lambda}{\lambda^3} \int_0^{r_{\mathrm{Core}}} N_3(r) \boldsymbol{f}_{\mathrm{Er}}(r) \times 2\pi r dr. \tag{4}$$

Here $\boldsymbol{K}$—is the array with degrees of degeneracy of LP modes, taking into account the polarization. The multiplication of two arrays ($\boldsymbol{K}$ and $\boldsymbol{f}_{Er}$) is performed elementwisely.

2.3 Rate equations in Yb/Er doped active fiber

In this case, the stimulated transitions probabilities W_{ij} per unit of time between energy levels i and j are equal to:

$$\begin{cases} W_{01} = \int \left(I^{\mathrm{f}}_{\mathrm{p}} + I^{\mathrm{b}}_{\mathrm{p}} + I^{\mathrm{f}}_{\mathrm{aseYb}} + I^{\mathrm{b}}_{\mathrm{aseYb}}\right)\sigma_{01}\frac{\lambda}{hc}d\lambda; \\ W_{10} = \int \left(I^{\mathrm{f}}_{\mathrm{p}} + I^{\mathrm{b}}_{\mathrm{p}} + I^{\mathrm{f}}_{\mathrm{aseYb}} + I^{\mathrm{b}}_{\mathrm{aseYb}}\right)\sigma_{10}\frac{\lambda}{hc}d\lambda; \\ W_{23} = \int sum\left(\boldsymbol{I}^{\mathrm{f}}_{\mathrm{s}} + \boldsymbol{I}^{\mathrm{b}}_{\mathrm{s}} + \boldsymbol{I}^{\mathrm{f}}_{\mathrm{aseEr}} + \boldsymbol{I}^{\mathrm{b}}_{\mathrm{aseEr}}\right)\sigma_{23}\frac{\lambda}{hc}d\lambda; \\ W_{32} = \int sum\left(\boldsymbol{I}^{\mathrm{f}}_{\mathrm{s}} + \boldsymbol{I}^{\mathrm{b}}_{\mathrm{s}} + \boldsymbol{I}^{\mathrm{f}}_{\mathrm{aseEr}} + \boldsymbol{I}^{\mathrm{b}}_{\mathrm{aseEr}}\right)\sigma_{32}\frac{\lambda}{hc}d\lambda. \end{cases} \tag{5}$$

Here c is the speed of light in vacuum, h is Planck's constant, the *sum* function designates the summation of all elements of the array.

Rate equations have different forms for different types of ions, so they can be divided into a number of independent subsystems. For the determination of a stationary solution the condition that all time derivatives are equal to zero is used.

The system of the rate equations for isolated Yb ions is:

$$\begin{cases} \frac{\partial \overline{N}_0}{\partial t} = W_{10}\overline{N}_1 - W_{01}\overline{N}_0 + A_{10}\overline{N}_1 = 0; \\ \overline{N}_{\mathrm{Yb}} - \overline{N}_0 - \overline{N}_1 = 0. \end{cases} \tag{6}$$

This system is linear and can be solved using ordinary algebraic transformations.

The system of the rate equations for non-clustered Er ions and non-isolated Yb ions interacting with them, including ET and SET processes, as well as the upconversion, has the following form [6, 8]:

$$\begin{cases} \frac{\partial \hat{N}_0}{\partial t} = W_{10}\hat{N}_1 - W_{01}\hat{N}_0 + A_{10}\hat{N}_1 + C_{\mathrm{ET}}\hat{N}_1\hat{N}_2 \\ -C_{\mathrm{ET}}\hat{N}_0\hat{N}_4 + C_{\mathrm{SET}}\hat{N}_1\hat{N}_3 = 0; \\ \hat{N}_{\mathrm{Yb}} - \hat{N}_0 - \hat{N}_1 = 0; \\ \frac{\partial \hat{N}_2}{\partial t} = W_{32}\hat{N}_3 - W_{23}\hat{N}_2 + A_{32}\hat{N}_3 - C_{\mathrm{ET}}\hat{N}_1\hat{N}_2 \\ +C_{\mathrm{UC}}\left(\hat{N}_3\right)^2 + C_{\mathrm{ET}}\hat{N}_0\hat{N}_4 = 0; \\ \frac{\partial \hat{N}_3}{\partial t} = W_{23}\hat{N}_2 - W_{32}\hat{N}_3 + A_{43}\hat{N}_4 \\ -A_{32}\hat{N}_3 - 2C_{\mathrm{UC}}\left(\hat{N}_3\right)^2 - C_{\mathrm{SET}}\hat{N}_1\hat{N}_3 = 0; \\ \hat{N}_{\mathrm{Er}} - \hat{N}_2 - \hat{N}_3 - \hat{N}_4 = 0. \end{cases} \tag{7}$$

Here, terms $W_{ij}\hat{N}_i$ are responsible for stimulated transitions between the corresponding energy levels, $A_{ij}\hat{N}_i$—for spontaneous transitions, $C_{\mathrm{ET}}\hat{N}_{\mathrm{i}}\hat{N}_{\mathrm{j}}$ and $C_{\mathrm{SET}}\hat{N}_1\hat{N}_3$—for first and secondary energy transfer between Yb and Er ions, $C_{\mathrm{UC}}\left(\hat{N}_3\right)^2$—for upconversion process in Er subsystem.

Using substitution method after simple but cumbersome algebraic transformations we can obtain the system of equations, first of which is a fourth-degree algebraic equation for only one variable $\hat{N}_3$:

$$\begin{cases} f_4\left(\hat{N}_3\right)^4 + f_3\left(\hat{N}_3\right)^3 + f_2\left(\hat{N}_3\right)^2 + f_1\hat{N}_3 + f_0 = 0; \\ \hat{N}_4 = \frac{a_3\left(\hat{N}_3\right)^3 + a_2\left(\hat{N}_3\right)^2 + a_1\hat{N}_3 + a_0}{b_1 \times \hat{N}_3 + b_0}; \\ \hat{N}_2 = \hat{N}_{\mathrm{Er}} - \hat{N}_3 - \hat{N}_4; \\ \hat{N}_1 = \hat{N}_{\mathrm{Yb}} \times \frac{W_{01} + C_{\mathrm{ET}}\hat{N}_4}{W_{01} + W_{10} + A_{10} + C_{\mathrm{ET}}\left(\hat{N}_{\mathrm{Er}} - \hat{N}_3\right) + C_{\mathrm{SET}}\hat{N}_3}; \\ \hat{N}_0 = \hat{N}_{\mathrm{Yb}} - \hat{N}_1. \end{cases} \tag{8}$$

The values of the coefficients of the fourth degree equation for $\hat{N}_3$ are given in Table 1. A solution for the fourth-degree algebraic equation can be written using the Ferrari method, which reduces a fourth-degree equation to one third-degree equation and two quadratic equations. In turn, the third-degree equation can be solved using Vieta's trigonometric formulas. After finding $\hat{N}_3$ it is possible to find other concentrations $\hat{N}_4$,$\hat{N}_2$,$\hat{N}_1$,$\hat{N}_0$ sequentially using (8).

The system of the rate equations for clustered Er ions and non-isolated Yb ions interacting with them:

$$\begin{cases} \frac{\partial \check{N}_0}{\partial t} = W_{10}\check{N}_1 - W_{01}\check{N}_0 + A_{10}\check{N}_1 \\ +C_{\mathrm{ET}}\check{N}_1\left(2R_0 + R_1\right) = 0; \\ \check{N}_{\mathrm{Yb}} - \check{N}_0 - \check{N}_1 = 0; \\ \frac{\partial R_0}{\partial t} = W_{32}R_1 - 2W_{23}R_0 + A_{32}R_1 - 2C_{\mathrm{ET}}\check{N}_1R_0 = 0; \\ R_{\mathrm{Er}} - R_0 - R_1 = 0. \end{cases} \tag{9}$$

Here $R_{\mathrm{Er}} = \check{N}_{\mathrm{Er}}/2$—total cluster concentration, R_0, R_1 – concentrations of the clusters in the ground and excited states, respectively. In this case, $\check{N}_2 = R^{\mathrm{Er}} + R_0$, $\check{N}_3 = R^{\mathrm{Er}} - R_0$. The system of equations can be reduced to a quadratic equation that has an analytical solution in the same way as it was made for the system of Eq. (7).

Table 1 List of found parameters

Parameter	Value
a_0	$C_{ET} \times W_{01} \times \hat{N}_{Yb} \times \hat{N}_{Er}$
a_1	$W_{01} \times \hat{N}_{Yb} \times (C_{SET} - C_{ET})$
a_2	$C_{UC} \times (W_{01} + W_{10} + A_{10} + C_{ET} \times N_1^{Er})$
a_3	$C_{UC} \times (C_{SET} - C_{ET})$
b_0	$A_{43} \times C_{ET} \times \hat{N}_{Er} + (A_{43} + C_{ET} \times \hat{N}_{Yb}) \times (W_{01} + W_{10} + A_{10})$
b_1	$A_{43} \times (C_{SET} - C_{ET})$
c_0	$W_{23} \times \hat{N}_{Er} \times (W_{01} + W_{10} + A_{10} + C_{ET} \times \hat{N}_{Er})$
c_1	$-C_{SET} \times W_{01} \times \hat{N}_{Yb} - (W_{23} + W_{32} + A_{32}) \times (W_{01} + W_{10} + A_{10} + C_{ET} \times \hat{N}_{Er}) + W_{23} \times \hat{N}_{Er} \times (C_{SET} - C_{ET})$
c_2	$-2 \times C_{UC} \times (W_{01} + W_{10} + A_{10} + C_{ET} \times \hat{N}_{Er}) - (C_{SET} - C_{ET}) \times (W_{23} + W_{32} + A_{32})$
c_3	$-2 \times C_{UC} \times (C_{SET} - C_{ET})$
d_0	$(W_{23} - A_{43}) \times (W_{01} + W_{10} + A_{10} + C_{ET} \times \hat{N}_{Er})$
d_1	$C_{ET} \times C_{SET} \times \hat{N}_{Yb} + (W_{23} - A_{43}) \times (C_{SET} - C_{ET})$
f_0	$d_0 \times a_0 - b_0 \times c_0$
f_1	$d_1 \times a_0 + d_0 \times a_1 - b_1 \times c_0 + b_0 \times c_1$
f_2	$d_1 \times a_1 + d_0 \times a_2 - b_1 \times c_1 + b_0 \times c_2$
f_3	$d_1 \times a_2 + d_0 \times a_3 - b_1 \times c_2 + b_0 \times c_3$
f_4	$d_1 \times a_3 - b_1 \times c_3$

As we know, the active ions transitions between different energy levels, specified by the probabilities W_{ij} and A_{10}, A_{32}, determine the change in the optical power, passing through active medium. The system of the equations describing the evolution of optical power in each mode has the following form:

$$\begin{cases} \pm\frac{\partial P_p^{f/b}}{\partial z} = P_p^{f/b}\frac{\pi(r_{core})^2}{\pi(r_{clad})^2}\left(\sigma_{10}\frac{\int_0^{r_{core}} N_1(r)\times 2\pi r dr}{(r_{Core})^2} - \sigma_{01}\frac{\int_0^{r_{core}} N_0(r)\times 2\pi r dr}{(r_{Core})^2}\right); \\ \pm\frac{\partial P_{aseYb}^{f/b}}{\partial z} = P_{aseYb}^{f/b}\left(\sigma_{10}\frac{\int_0^{r_{core}} N_1\times 2\pi r dr}{(r_{Core})^2} - \sigma_{01}\frac{\int_0^{r_{core}} N_0(r)\times 2\pi r dr}{(r_{core})^2}\right) + \frac{\partial P_{seYb}^{f/b}}{\partial z}; \\ \pm\frac{\partial \boldsymbol{P}_s^{f/b}}{\partial z} = \boldsymbol{P}_s^{f/b}\left(\sigma_{32}\int_0^{r_{core}} N_3(r)\boldsymbol{f}_{Er}\times 2\pi r dr - \sigma_{23}\int_0^{r_{core}} N_2(r)\boldsymbol{f}_{Er}\times 2\pi r dr\right); \\ \pm\frac{\partial \boldsymbol{P}_{aseEr}^{f/b}}{\partial z} = \boldsymbol{P}_{aseEr}^{f/b}\left(\sigma_{32}\int_0^{r_{core}} N_3(r)\boldsymbol{f}_{Er}\times 2\pi r dr - \sigma_{23}\int_0^{r_{core}} N_2(r)\boldsymbol{f}_{Er}\times 2\pi r dr\right) + \frac{\partial \boldsymbol{P}_{seEr}^{f/b}}{\partial z}. \end{cases} \quad (10)$$

Here the terms $\partial \boldsymbol{P}_{seYb}^{f/b}/dz$ and $\partial \boldsymbol{P}_{seEr}^{f/b}/dz$ are given by the Eqs. (3) and (4), correspondingly. In the case of the amplifier, the following boundary conditions were used:

$$\begin{cases} P_p^f\big|_{z=0} = J_p^f, \quad P_p^b\big|_{z=L} = J_p^b, \\ P_{aseYb}^f\big|_{z=0} = 0, \quad P_{aseYb}^b\big|_{z=L} = 0, \\ \boldsymbol{P}_s^f\big|_{z=0} = \boldsymbol{J}_s, \quad \boldsymbol{P}_s^b\big|_{z=L} = 0, \\ \boldsymbol{P}_{aseEr}^f\big|_{z=0} = 0, \quad \boldsymbol{P}_{aseEr}^b\big|_{z=L} = 0. \end{cases} \quad (11)$$

Here $z=0$ corresponds to the point of the signal input, L—length of active fiber, J_p^f and J_p^b—pump powers launched from different sides of the amplifier, $\boldsymbol{J}_s$—array of the input signal power, the components of which characterize the power in each mode of the fiber.

For solving the presented system of nonlinear differential equations, the *relaxation method* was used, which is based on the sequential solution of the Cauchy problems for the radiation propagating in one direction and for the radiation propagating in the opposite direction. At each new iteration, in order to find the solution for the radiation propagating in one direction we used the solution found at the previous iteration for the radiation propagating in the opposite direction. About 10–20 iterations made it possible to find the stationary solution.

In this section, we have introduced a most complete model that describes Yb/Er-doped multimode fibers, compared to those presented in literature. This model considers

not only various interaction mechanisms of active ions with each other, but also the presence of clustered and isolated active ions.

3 Experiment

3.1 Measurements of the luminescence decay of active ions

In order to complete the model, we should determine the coefficients C_{ET}, C_{SET}, C_{UC}. It is known, that these coefficients determine the dynamics of the population inversion change in active medium depending on pump power [6]. The luminescence power at the amplifier output is proportional to the share of excited active ions, $\left(\overline{N}_1 + \hat{N}_1\right)/\left(\overline{N}_{Yb} + \hat{N}_{Yb}\right)$ for Yb ions and $\hat{N}_3/\hat{N}_{Er}$ for Er ions, averaged over the cross section and the length of the active fiber [13]. Therefore, by measuring the luminescence decay, the values of these parameters can be determined.

The block scheme of the experimental setup is shown in Fig. 2a. In all our experiments we used Yb/Er-doped active fiber with Yb ion concentration $6.2{\cdot}10^{26}$ m^{-3} and Er ion concentration $1.3{\cdot}10^{25}$ m^{-3}, the diameter of active core was 15 µm. The calculated number of transverse LP modes in the core without taking into account its polarization degeneracy was 16 at ~ 1060 nm (multi-mode regime), and 6 (few-mode regime) at 1550 nm. Therefore, we can justify the use of different forms of Eqs. (3) and (4) for different ASE wavelengths. In Table 2 absorption cross sections, measured from absorption of low power supercontinuum radiation in fiber specimen, and emission cross sections, calculated through McCumber theory, are shown. The generator Tektronix AFG3052C provided the rectangular electrical pulses with 20 ms duration and 10 Hz repetition rate. The pulse rise and fall times were 7 ns. These pulses powered the semiconductor laser diode based on GaAs heterostructures (~ 975 nm wavelength) with 125 µm multimode fiber output. The duration of the fronts of the optical pulses from the diode did not exceed 1 µs. The backward luminescence signal spectrally separated using Wave Division Multiplexor (WDM) was collected by the photodiode connected to the Tektronix DPO 3054 oscilloscope for further processing. Despite the fact that the losses of multimode pump radiation in the SMF-28 fiber were high, the remaining radiation was sufficient to create the required population inversion in the 10 mm segment of the active fiber.

Table 2 Emission and absorption cross-sections

Parameter	Absorption	Emission
Yb^{3+} ions @962 nm	$2.7{\cdot}10^{-25}$ m^2	$1.8{\cdot}10^{-25}$ m^2
Yb^{3+} ions @975 nm	$1.3{\cdot}10^{-24}$ m^2	$1.4{\cdot}10^{-24}$ m^2
Er^{3+} ions @1550 nm	$3.3{\cdot}10^{-25}$ m^2	$4.4{\cdot}10^{-25}$ m^2

The goal of the experiment was to measure the decay of the luminescence power immediately after the turning off the pump diode. To find the correspondence between measured luminescence signal and share of excited active ions the following algorithm was used. We know, that the decay curve of the share of excited ions coincides with the decay curve of luminescence, so it was necessary to find the initial value of the share of excited ions immediately after the end of the pump pulse. The pulse duration 20 ms allows to achieve a stationary state in the Yb/Er medium after turning on of pumping, what is confirmed by the measured oscillograms—the luminescence signal reached a plateau during 20 ms.

Therefore, it is possible to use the stationary solutions of the rate equations to find the initial value of the share of excited ions. For the given set of the coefficients C_{ET}, C_{SET}, C_{UC}, A_{10}, A_{32} values the stationary analytical solution of

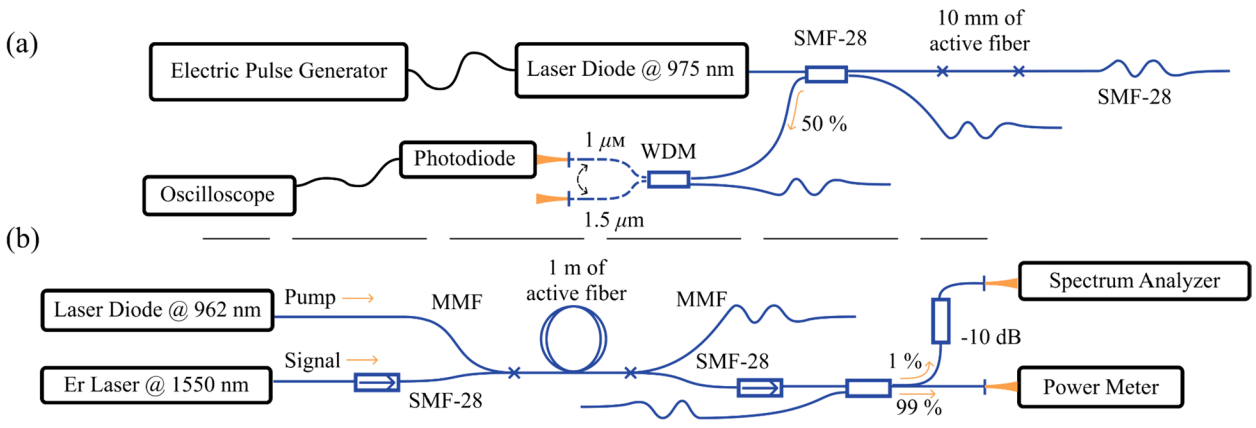

Fig. 2 **a** Scheme of the experimental setup for measuring the luminescence decay of Yb and Er ions. **b** Scheme of the experimental setup for measuring the output power and optical spectrum of an ytterbium-erbium fiber amplifier. *MMF* multimode fiber

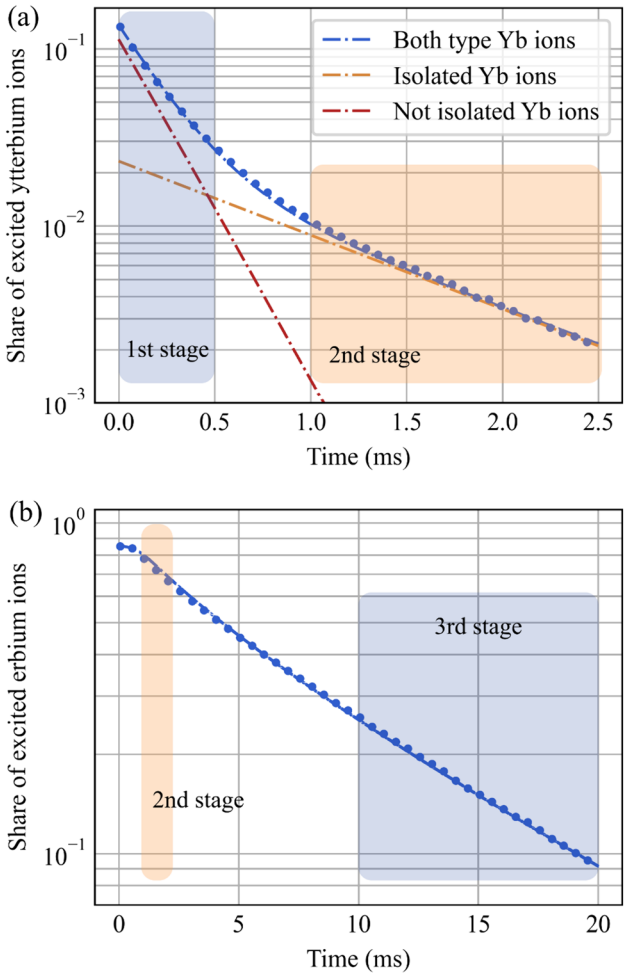

Fig. 3 Dependence of the share of excited ions on time after switching off the pump pulse (pump power 3.7 mW) for **a** Yb ions (isolated and not isolated), **b** Er ions. Dash-dotted lines show simulation results, dots—experimental results

the systems of equations for isolated Yb ions (6) and for non-isolated Yb ions interacting with Er ions (7) was found. The obtained decays of the share of excited Yb and Er ions just after the pump pulse end are shown in Fig. 3.

To analyze the evolution of the share of excited ions in the subsystems of Yb and Er ions, the Eqs. (6, 7) were solved numerically using the 4th order Runge–Kutta method. Since the process is non-stationary, the derivatives in the Eqs. (6, 7) are not equal to zero. The coefficients W_{01}, W_{10}, W_{23}, W_{32} are equal to zero, since there is no pump and signal. ASE was neglected, since the length of the active fiber was only 10 mm. The stationary solution mentioned above was used as the initial condition for solving the Cauchy problem.

The evolution of the share of excited isolated Yb ions is described by the equation:

Table 3 List of found parameters

Parameter	Found value	Literature
C_{ET}	$(1.6–2.0)\cdot10^{-21}$ m^3/s	$(2–3)\cdot10^{-20}$ m^3/s [11] $(2–4)\cdot10^{-22}$ m^3/s [6] $(0.7–1.4)\cdot10^{-22}$ m^3/s [15] $4.4\cdot10^{-22}$ m^3/s [9] $2.4\cdot10^{-22}$ m^3/s [16]
C_{SET}	$(1.0–3.0)\cdot10^{-22}$ m^3/s	$(1.5–4)\cdot10^{-22}$ m^3/s [6] $7.3\cdot10^{-23}$ m^3/s [9]
C_{UP}	$(5.2–5.6)\cdot10^{-24}$ m^3/s	$(3–15)\cdot10^{-24}$ m^3/s [6] $(0.8–1.7)\cdot10^{-24}$ m^3/s [15] $3\cdot10^{-24}$ m^3/s [16] $9.1\cdot10^{-23}$ m^3/s [9]

$$\overline{N}_0(t) = \overline{N}_{Yb} - \left(\overline{N}_{Yb} - \overline{N}_0(0)\right)e^{-A_{10}t}. \quad (12)$$

After switching off the pump, for up to 0.5 ms (first stage) the share of excited ions in the Yb subsystem is quite large, so the SET process prevails. Since almost all Er ions are in the excited state, the ET process is negligibly weak. For the same reason, the share of excited ions in the erbium subsystem remains stationary. It is clear that the approximation of this section gives the value of C_{SET}. Indeed, basing on the first two equations of the system (7), we can see that the slope of the Yb ion decay curve is $1/(A_{10} + C_{SET} \times \hat{N}_{Er})$ under the assumption that the share of excited ions in the Er subsystem is 100%.

In the time interval from 1.0 ms to 2.5 ms (second stage), the $^2F_{5/2}$ energy level of non-isolated Yb ions is empty; therefore, the share of excited ions decay in Fig. 3a is governed by the isolated Yb ions. The decay time of the population inversion (i.e. the slope of the curve) coincides with the lifetime of the $^2F_{5/2}$ energy level due to the spontaneous transitions ($1/A_{10}$ ~1 ms). The point of the transition between first and second stages to the time span, where the luminescence from the isolated Yb ions becomes dominant, determines its fraction, which was estimated to be 8%. At this time moment, Er ions begin to evolve independently, with the share of excited ions decay time being about $1/(A_{32} + C_{UC} \times \hat{N}_{Er})$. The slope approximation in this time span gives the value of C_{UC} coefficient.

At the third stage (from 10 to 20 ms) the share of excited ions in the Er subsystem is so small that the contribution of the upconversion process can be neglected. Then the slope of the decay curve in Fig. 3b is determined by the lifetime of $^4I_{13/2}$ level ($1/A_{32}$ ~10 ms).

It should be noted, that the clustering of Er ions was not taken into account when simulating the luminescence decay. Indeed, in such experiment the clustered Er ions behave similarly to ordinary ions with the only difference—its share of excited ions did not exceed 50%, while the lifetimes and the excitation transfer rates where the same. According to our

calculations, for $k_{Cl}=5\%$ the error is about 2.5%; this value hardly exceeds the accuracy of the conducted experiments.

Thus, the presented analysis made it possible to determine all the necessary coefficients (see Table 3) with the exception of C_{ET} and k_{Cl}.

3.2 Non-saturable signal absorption in the amplifier

In the paper [4] the method for the determination of the degree of Er ions clustering was proposed. It is known, that, in the absence of the clustered ions, with the increase of the input signal passing through the unpumped active medium the population inversion eventually achieves the level at which the stimulated absorption rate is compensated by spontaneous and stimulated emission. As a result, the signal passes through the medium without power loss. However, this is not observed in active media with the considerable degree of ion clustering. The absorption does not saturate, because clusters, in which two ions are excited, relax very quickly into the state in which only one ion is excited. So that, this effect makes it possible to determine accurately the degree of clustering k_{Cl}.

By measuring the ratio of the absorption coefficients of the powerful and weak signals at the amplifier input, it is possible to calculate k_{Cl} [4]:

$$\frac{Abs_{ns}}{Abs_{ss}} = k_{Cl} \times \frac{\sigma_a}{2\sigma_a + \sigma_e}. \quad (13)$$

Here Abs_{ss} [dB/m]—weak signal absorption (when the inversion is zero), Abs_{ns} [dB/m]—non-saturable absorption of the powerful signal, when only the subsystem of clustered Er ions, in which the inversion cannot be greater than 0.5, can absorb radiation. This method suggested in [4] for Er-doped medium also suits for the case of Yb/Er-doped medium. Firstly, since signal wavelength is about 1550 nm, Yb ions do not have corresponding transitions between energy levels. Secondly, Er ions cannot transfer energy to Yb ions from $^4I_{13/2}$ energy level. And $^4I_{11/2}$ level is empty without pumping. Therefore, Yb ions do not play significant role in such measurements.

We estimated the clustering degree in the studied active fiber by measuring the signal transmission in the fiber section with a length of 1 m in the absence of the pump. The signal wavelength was 1567 nm, $\sigma_a = 0.14$ pm^2, $\sigma_e = 0.26$ pm^2. It turned out, that the absorption of the weak signal (-20 dBm to -10 dBm) was $Abs_{ss} = (-8.72 \pm 0.05)$ dB, and the absorption of the powerful signal ($+25$ dBm to $+33$ dBm) was $Abs_{ns} = (-0.11 \pm 0.03)$ dB. Hence, we obtained that k_{Cl} in the fiber under study was 4–6%.

3.3 Power and spectral characteristics of YEDFA

The final goal was the selection of one set of the parameters C_{ET}, C_{SET}, C_{UC}, k_{Cl} that provides the maximum possible agreement between the experimental and modeling results in the entire set of experiments at once. A good way to verify the correctness of the model is to check the agreement between the experimental data and the calculated parameters, such as the output power and the emission spectrum of the YEDFA. The scheme of the experimental setup is shown in Fig. 2b. YEDFA was assembled employing a GT-wave fiber, consisting of the few-mode Yb/Er-doped waveguide, that was used in the previous experiments, and the multimode waveguide, where pump radiation propagated. These two waveguides were in optical contact with each other covered with a common polymer coating.The maximum power of the pump radiation from the laser diode at ~ 962 nm wavelength was 2 W. The length of the active fiber was 1 m. To measure the output power and to control the spectral characteristics of the output radiation of the signal the Coherent PM-USB PM3 thermal power meter and the Yokogawa AQ6370D spectrum analyzer were used, respectively.

Simulations were carried out on the basis of the Eqs. (3–11) considering 8% of the isolated Yb ions and 5% of the clustered Er ions. Amplifier has been divided into 100 parts ($\Delta z = 1$ cm) along longitudual direction and into 40 parts along radial direction. The step of spectral division was 0.02 nm for signal (1549.4–1550.6 nm) and pump (958–966 nm) radiation and 0.7 nm for ASE (1000–1110 nm and 1530 – 1555 nm).

The dependence of the output power of the amplifier on pump is shown in Fig. 4a. The input signal power was varied from 0.1 to 6.8 mW. Due to the large difference in output power values (two orders of magnitude), we used a logarithmic scale for the y-axis. The measured optical spectra of the output radiation confirm the absence of the parasitic generation at wavelengths near 1.0 μm. The best agreement between the experimental and calculated results was achieved by varying two parameters—C_{ET}, C_{SET}. The final set of the values of these parameters is presented in Table 3.

Equally important is how accurately the proposed model describes the spectral characteristics of the output radiation. For this purpose, the optical spectrum was also measured. The experimental and calculated spectra of the output radiation are shown in Fig. 4b. The measurements were carried out at the output of the single-mode passive SMF-28 fiber, which was used to connect investigated active fiber with the measuring equipment. Since the mode field diameters of the fundamental modes of the active fiber and SMF-28 fiber were matched, it is necessary to analyze the characteristics of only the fundamental mode radiation. It can be seen, that

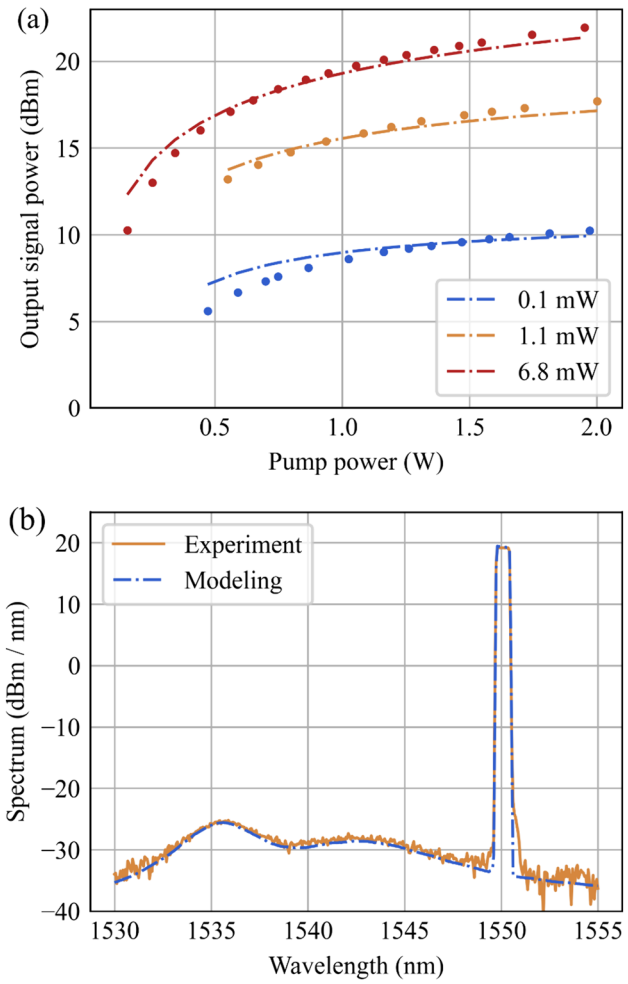

Fig. 4 Characteristics of the output radiation of the YEDFA: **a** output power (for different input signal powers), **b** optical spectrum (for pump power 0.6 W and input signal power 6.8 mW). Dash-dotted lines show simulation results, dots—experimental results

the calculated and experimentally measured spectra of the amplifier are in very good agreement.

4 4. Conclusions

In this work, the most complete model of a few-mode YEDFA was introduced. It takes into account effects of the secondary energy transfer and the upconversion, ASE from Yb and Er ions, the presence of several transverse radiation modes, the existence of the isolated Yb ions and the clustered Er ions. The fact that the part of the rate equations was solved analytically, which was not previously implemented in literature, made it possible to significantly simplify and accelerate the numerical calculations.

Since it was difficult to determine so many variables from single measurement all at once, we defined them one by one, selecting the optimal sequence of experiments. To achieve this, it was important to ensure that parameters that were not calculated in a particular experiment did not have a significant impact on its result. Finally, the complete series of the conducted experiments made it possible to determine the full set of the characteristics of the active medium (Table 3). Thus, this approach made it possible to define a set of parameters that satisfied not only single experiments, but their entire set as a whole, providing an additional check of self-consistency and universality. The determination accuracy of the parameters of the medium is limited both by the errors of the characteristics of the optical fiber (the refractive index profile, the doping profile) and by the errors of the experimental data.

Obtained parameters are consistent with the values given in the scientific literature [6, 9, 11, 15, 16]. At the same time, it should be taken into account, that these parameters strongly depend on the concentrations of active ions, the doping profile of the core, fiber drawing technology, the uniformity of the fiber and other parameters. So, the direct comparison of the results is improper.

Introduced model allows one to calculate both the power and the spectral characteristics of YEDFA amplifiers, as well as the nonstationary dynamics of the population inversion and the luminescence of active ions. Using this model, it is possible to calculate the main characteristics of both single-mode and few-mode YEDFA's depending on various parameters of the active fiber. It also makes it easier to select the required concentrations of active ions, the geometry and the length of active fibers for each specific task. By changing the boundary conditions (11) for the rate equations, it is possible to apply presented model for the calculation of the characteristics of ytterbium-erbium high-power lasers as well.

Acknowledgements Authors thanks Alexei V. Konyashkin from Kotelnikov FIRE RAS for the help in editing the text.

Author contributions Foat Iakupov, Maksim Chernikov, Renat Shaidullin performed literature review.Foat Iakupov, Maksim Chernikov, Andrey Baranov prepared the theoretical model based on scientific literature.Foat Iakupov, Maksim Chernikov carried out the experiments with the ytterbium-erbium fiber amplifier.Foat Iakupov prepared Python scripts for calculations, drawed all Figures.Foat Iakupov, Maksim Chernikov performed general analysis of experimental and theoretical results, made conclusions and general results.Foat Iakupov, Renat Shaidullin wrote the main manuscript text.All authors reviewed the manuscript.

Data availability No datasets were generated or analysed during the current study.

Declarations

Conflict of interest The authors declare no conflict of interest.

References

1. M. Federighi, F. Di Pasquale, The effect of pair-induced energy transfer on the performance of silica waveguide amplifiers with high Er^{3+}/Yb^{3+} concentrations. IEEE Photonics Technol. Lett. **7**(3), 303–305 (1995)
2. N.V. Kiritchenko et al., Effect of ytterbium co-doping on erbium clustering in silica-doped glass. Laser Phys. **25**, 025102 (2015)
3. S. Taccheo et al., Diode-pumped bulk erbium-ytterbium lasers. Appl. Phys. B **63**, 425–436 (1996)
4. P. Myslinski, D. Nguyen, J. Chrostowski, Effects of concentration on the performance of erbium-doped fiber amplifiers. J. Lightwave Technol. **15**(1), 112–120 (1997)
5. A. Giaquinto et al., Particle swarm optimization-based approach for accurate evaluation of upconversion parameters in Er^{3+}-doped fibers. Opt. Lett. **36**(2), 142–144 (2011)
6. G.A. Sefler et al., Secondary energy transfer and nonparticipatory Yb^{3+} ions in Er^{3+}-Yb^{3+} high-power amplifier fibers. J. Opt. Soc. Am. B **21**, 1740–1748 (2004)
7. M. Bolshtyansky, I. Mandelbaum, F. Pan, Signal excited-state absorption in the L-band EDFA: Simulation and measurements. J. Lightwave Technol. **23**(9), 2796–2799 (2005)
8. M. Karasek, Optimum design of Er^{3+}-Yb^{3+} codoped fibers for large-signal high-pump-power applications. IEEE J. Quantum Electron. **33**(10), 1699–1705 (1997). https://doi.org/10.1109/3.631268
9. L. Mescia et al., Optimization of the design of high power Er^{3+}/Yb^{3+}-codoped fiber amplifiers for space missions by means of particle swarm approach. IEEE J. Sel. Top. Quantum Electron. **20**(5), 494–491 (2014)
10. L. Mescia et al., Temperature dependent modelling of cladding-pumped Er^{3+}/Yb^{3+}-codoped fiber amplifiers for space applications. J. Lightwave Technol. **36**(17), 3594–3602 (2018)
11. L. Dong et al., Modeling Er/Yb fiber lasers at high powers. Opt. Express **28**, 16244–16255 (2020)
12. D. Richardson, J. Fini, L. Nelson, Space-division multiplexing in optical fibres. Nat. Photonics **7**, 354–362 (2013)
13. E. Desurvire, *Erbium-Doped Fiber Amplifiers: Principles and Applications* (Wiley InterScience, 1994)
14. G. Agrawal, *Nonlinear Fiber Optics* (Academic Press, 1995), pp.34–36
15. J. Philipps et al., Energy transfer and upconversion in erbium–ytterbium-doped fluoride phosphate glasses. Appl. Phys. B **74**, 233–236 (2002)
16. Q. Han, J. Ning, Z. Sheng, Numerical investigation of the ASE and power scaling of cladding-pumped Er–Yb codoped fiber amplifiers. IEEE J. Quantum Electron. **46**(11), 1535–1541 (2010)